Proceedings of the
46th IEEE Conference on Decision and Control
New Orleans, LA, USA, Dec. 12-14, 2007

WePI21.7

Robust feasibility for control of water flow in a reservoir-canal system

Saurabh Amin[†], Alexandre M. Bayen[†], Laurent El Ghaoui[‡] and Shankar Sastry[‡]

Abstract— A robust control problem for distant downstream control of a reservoir-canal system modeled by Saint-Venant equations is investigated. The problem is to regulate the release of water at the upstream end such that the measured water level (or stage) at the downstream end does not deviate outside of pre-scribed bounds under the effect of downstream perturbations. Under the assumption of small perturbations, the Saint-Venant model is linearized around a steady state flow. The resulting linear model is discretized to obtain a linear state-space model using a method of characteristics based numerical scheme. For the state space model, the control is the upstream discharge deviation, the disturbance is the downstream discharge deviation and the output is the downstream stage deviation; the deviations are defined with respect to the steady state. The sets of admissible control, disturbance and output trajectories are modeled by polytopes. It is shown that the control problem can be formulated as a robust feasibility problem. Using linear programming duality, conditions for existence of a robustly feasible solution are derived. These conditions, being affine in the control variables, are checked using linear programming. The proposed method is applied to control a typical reservoir-canal system.

I. INTRODUCTION

Open-channel hydraulic systems are central to a variety of human needs such as irrigation, power generation and flood-control. Since water is increasingly becoming a precious resource, efficient management of irrigation systems has become a crucial issue. Historically, irrigation systems around the world were manually operated and users withdrew a pre-scheduled amount of water which was within the capacity limits of the system [1]. The control policy used was local upstream control, where the downstream hydraulic structure is used to control water level (stage) just upstream. Although this control policy is easy to implement, it does not support on-demand water supply and may lead to high operational losses.

Another well-known canal control policy is the distant downstream control wherein, the upstream flow is controlled to meet desired downstream demand [2]. This policy supports more effective utilization but may compromise on the efficiency with respect to the users if the downstream demand is not met sufficiently soon. Implementation of a distant downstream control policy that is both user efficient and resource effective is complicated and usually requires design of automatic controllers.

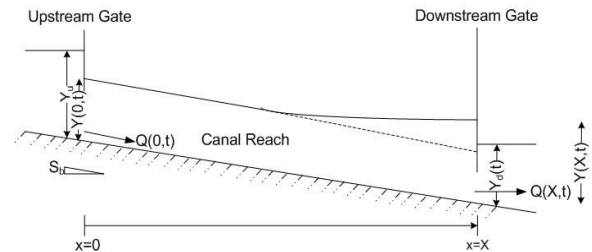This article focuses on the distant downstream control of

Fig. 1. A reservoir-canal system.

a reservoir-canal system as shown in Figure 1 modeled by Saint-Venant equations. These equations are quasi-linear, hyperbolic *partial differential equations* (PDEs). They describe the dynamics of one-dimensional flow in open-channels hydraulic systems and have been widely used in hydraulics [3]. The flow conditions are assumed to be subcritical - that is, the gravity wave speed is higher than the flow speed. The objective is to find a suitable control that will regulate the upstream discharge such that the downstream stage remains within prescribed bounds under the effect of downstream perturbations. These perturbations are typically caused by users withdrawing water at variable rates.

In order to achieve this objective, the Saint-Venant model is first linearized around a steady state, non-uniform flow in Section II. The linear PDE model is discretized to obtain a state space model using a *method of characteristics* (MOC) based explicit numerical scheme in Section III. For the state space model, upstream discharge from steady state is the control variable, the downstream discharge deviation is the disturbance variable and the downstream stage deviation is the output variable. The deviations are defined with respect to the steady state. Section IV models the set of admissible control, disturbance and output trajectories as convex polytopes. The robust feasibility problem is defined as that of finding an admissible control trajectory such that the output trajectory remains within the prescribed polytope under all admissible disturbances. Such a control trajectory, if it exists, is called *robustly feasible control*. It is shown that using *linear programming* (LP) duality, the existence of a robustly feasible control is equivalent to checking the feasibility of a set of *linear matrix inequalities* (LMIs). The case without control and the cases of feedforward and disturbance feedback controls are considered. Section V evaluates the performance by simulating the controlled flows for a typical reservoir-canal system. In Section VI, concluding remarks are drawn and scope of future work is discussed.

This article complements an already existing body of research regarding control of open-channel hydraulic systems, some of which include: PI control [4], ℓ_1 control [5], $\mathcal{H}_\infty$ control [6], LQ control [7],[8], model predictive control [9], control of nonlinear Saint-Venant PDE [10] based on a Riemann invariant approach and adjoint based optimization [11]. The method proposed in the present article differs from the literature in a number of aspects. To the best of our knowledge, in most of the earlier approaches based on the state space approximation, the discretization of the Saint-Venant model is followed by the linearization of the resulting non-linear algebraic equations [7]. A possible reason of this approach is that the state-space model was constructed from implicit finite-difference schemes such as the four-point Priessmann scheme [3]. On the other hand, in this article, the linearization of the Saint-Venant model around the steady state is followed by the discretization of the resulting linear PDE model. Our approach has the advantage that for the linear PDE model, the control, disturbance and output variables can be directly defined in terms of deviations from steady state. The linear PDE model can be discretized using a variety of numerical schemes to obtain a state space model. Even though the MOC-based numerical scheme does not allow large time steps for simulating the flow, the numerical solution converges to the actual solution of the linear PDE model as time step goes to zero.

Furthermore, since the conditions for existence of a robustly feasible control are affine in the control variables, these can be checked using *linear programming* (LP). This offers a computationally tractable solution to the robust feasibility problem.

II. MODELING RESERVOIR-CANAL SYSTEM

A. Saint-Venant Model

The Saint-Venant model for a rectangular cross-section is given by [3]:

$$TY_t + Q_x + w = 0 \tag{1}$$

$$Q_t + \left(\frac{Q^2}{TY} + \frac{gTY^2}{2} \right)_x + gTY(S_f - S_b) + wu' = 0 \tag{2}$$

for $(x,t) \in (0,X) \times \mathbb{R}^+$ with $Q(x,t)$ the discharge (m^3/s) across cross-section $A(x,t) = TY(x,t)$, $Y(x,t)$ the stage or water-depth (m), T the free surface width (m), $S_f(x,t)$ the friction slope, S_b the bed slope m/m, g the gravitational acceleration (m/s^2), w the distributed lateral-outflow per unit length of the channel (m^2/s) and u' the $x-$component of the lateral-outflow velocity (see Figure 1). Also, $V(x,t)$ the average velocity (m/s) in the cross-section A defined by $V = Q/A$ and $P(x,t)$ the wetted perimeter (m) defined by $P(x,t) = T + 2Y(x,t)$. Note that since the channel cross-section is assumed to be rectangular, the free surface width T is constant. The friction slope S_f is empirically modeled by the Manning-Strickler's formula [3]

$$S_f = \frac{Q^2 n^2}{A^2 R^{4/3}} \tag{3}$$

with n the Manning's roughness coefficient $(sm^{-1/3})$ and R the hydraulic radius (m), defined by $R = A/P$.

The boundary conditions are $Q(0,t) = Q_0(t)$ and $Q(X,t) = Q_X(t)$. This form of boundary conditions is best suited for canal control purposes, since they can be locally linked with the control structures via stage-discharge equations. The initial conditions are given by $Q(x,0), Y(x,0)$ for $x \in [0, X]$.

In this article, the upstream discharge $Q(0,t)$ is regulated to control the stage $Y(X,t)$ at the downstream end of the canal reach in response to the fluctuations in the downstream discharge $Q(X,t)$. We refer to $Q(0,t)$ as the *control action variable*, to $Q(X,t)$ as the *disturbance variable* and to $Y(x,t)$ as the *controlled variable*. It is assumed that $Y(X,t)$ can be measured by level sensors.

Remark 1: In practice, distant downstream canal control is achieved by controlling the upstream gate opening which in turn regulates the discharge released in the canal. The stage and discharge for the case of underflow sluice gate are related by $Q(0,t) = Q_0(t) = GW(t)(\Upsilon_u - Y(0,t))^{\frac{1}{2}}$ with G the coefficient depending on the gate design, W(t) the gate opening, Υ_u a fixed upstream water level. In this article, we do not explicitly consider gate opening as a control variable.

B. Steady state flow

Under constant boundary conditions, there exists a steady state solution of the Saint-Venant equations (1,2). We denote the variables corresponding to the steady state condition by $Q_0(x)$, $Y_0(x)$ etc. where $x \in (0,X)$ respectively. The Saint-Venant equations become

$$\frac{dQ_0(x)}{dx} = -w \tag{4}$$

$$\frac{dY_0(x)}{dx} = \frac{S_b - S_{f0}(x) + D_{l0} + \frac{F_0(x)^2 w Y_0(x)}{Q_0(x)}}{1 - F_0(x)^2} \tag{5}$$

with $C_0 = \sqrt{gY_0}$, $F_0 = V_0/C_0$, $V_0 = Q_0/A_0$, $D_{l0} = \frac{(V_0(x) - u')w}{T_0 Y_0 g}$. Here, C_0 is the gravity wave celerity, F_0 is the Froude number and D_{l0} is the dynamic contribution of lateral outflow, all under the steady state condition. These two equations define the steady state flow under lateral withdrawal. While $Q_0(x) = Q_0 - wx$ by the first equation, the second equation is solved for $Y_0(x)$ with boundary condition in terms of downstream elevation $Y_0(X)$. In this article, we assume the flow to be *sub-critical*, i.e., $F_0 < 1$.

C. Linearized Saint-Venant Model

Following [12], we obtain the linearized Saint-Venant model around the steady-state flow characterized by $Q_0(x)$ and $Y_0(x)$. Denoting the first-order perturbations in discharge and water level by $q(x,t)$ and $y(x,t)$ respectively, we have

$$Q(x,t) = Q_0(x) + q(x,t) \tag{6}$$

$$Y(x,t) = Y_0(x) + y(x,t) \tag{7}$$

Thus, $A(x,t) = A_0(x) + T_0 y(x,t)$ and $P(x,t) = P_0(x) + 2y(x,t)$. Note that T_0 was previously called T; the subscript 0 emphasizes that it is uniform. These equations

1572

are substituted in equations (1,2) and expanded in Taylor series. Neglecting higher order terms, a given term $f(Q, Y)$ of the Saint-Venant model can be written as: $f(Q, Y) = f(Q_0, Y_0) + (f_Q)_0 q + (f_Y)_0 y$ where, $(\cdot)_0$ indicates that all quantities are evaluated at steady state conditions. The linearized mass and momentum conservation equations become

$$T_0 y_t + q_x = 0 \tag{8}$$

$$q_t + 2V_0(x)q_x - \beta_0(x)q + \alpha_0(x)y_x - \gamma_0(x)y = 0 \tag{9}$$

with $\alpha_0(x)$, $\beta_0(x)$ and $\gamma_0(x)$ given by:

$$\alpha_0 = (C_0^2 - V_0^2)T_0 \tag{10}$$

$$\beta_0 = \frac{2g}{V_0}\left(F_0^2 \frac{w_0}{V_0 T_0} + F_0^2 \frac{dY_0}{dx} - S_{f0}\right) \tag{11}$$

$$\gamma_0 = gT_0\left(\kappa S_{f0} + S_b - \frac{2w_0}{V_0 T_0}F_0^2 - (1 + 2F_0^2)\frac{dY_0}{dx}\right) \tag{12}$$

with $\kappa = 7/3 - 8Y_0/(3P_0)$. In the above equations, the dependence on x is omitted for readability. Since the linearization is done around the steady state, the expressions for $\beta_0(x)$ and $\gamma_0(x)$ can be simplified further by substituting the expression for S_{f0} from equation (5) into (11,12), leading to

$$\gamma_0 = gT_0\left[(1 + \kappa)S_b - (1 + \kappa - (\kappa - 2)F_0^2)\frac{dY_0}{dx}\right]$$
$$+ gT_0\left[\kappa D_{l0} + (\kappa - 2)F_0^2\left(\frac{w_0}{V_0 T_0}\right)\right] \tag{13}$$

$$\beta_0 = -\frac{2g}{V_0}\left(S_b + D_{l0} - \frac{dY_0}{dx}\right) \tag{14}$$

The upstream and downstream boundary conditions are respectively

$$q(0, t) = u_0(t) \qquad\qquad q(X, t) = p_X(t) \tag{15}$$

where, $u_0(t)$ is the applied control and $p_X(t)$ is the disturbance. The initial conditions are given by

$$y(x, 0) = 0 \qquad q(x, 0) = 0 \qquad \forall x \in [0, X] \tag{16}$$

Finally, the measurement equation is simply

$$z(t) = y(X, t) \tag{17}$$

III. NUMERICAL SOLUTION OF LINEARIZED SAINT-VENANT MODEL

A. Method of Characteristics Solution

The characteristic form of the linearized Saint-Venant equations can be written as the following system of *ordinary differential equations* (ODEs):

$$\pm T_0(C_0(x) \mp V_0(x))\frac{dy}{dt} + \frac{dq}{dt} - (\gamma_0(x)y - \beta_0(x)q) = 0 \tag{18}$$

each, respectively, valid on

$$\frac{dx}{dt} = V_0(x) \pm C_0(x) \tag{19}$$

The solution of ODEs (19) gives a family of intersecting curves known as the left and right characteristics curves ($\mathcal{C}^+$ and $\mathcal{C}^-$). The four ODEs (18,19), known as the MOC solution, can be simultaneously solved to simulate the linearized Saint-Venant model starting from known initial and boundary conditions.
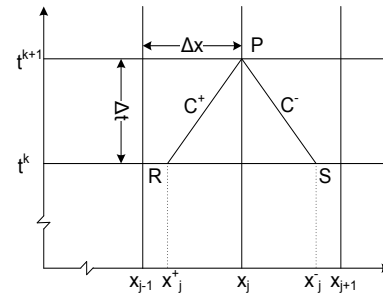

Fig. 2.　Solution by MOC.

Figure 2 shows the $x - t$ plane covered with a rectangular grid specified by lines of constant time and space steps. Consider the characteristic curves originating from points R and S and intersecting at point P. The region under the characteristic curves represents the domain of dependence of point P. Starting with known values of q and y at points R and S, the values at point P can be given by computed by solving equations (18). For upstream (resp. downstream) boundary, the pair of ODEs for $\mathcal{C}^-$ (resp. $\mathcal{C}^+$) is solved in conjunction with $q(0, t)$ (resp. $q(X, t)$). We now use the MOC to construct a numerical scheme to solve the linearized Saint-Venant model numerically.

B. Discretization Procedure

In order to numerically solve the MOC solution, we discretize the ODEs (18,19) using first-order integration method as used by [13]. The channel is discretized into a number of equal segments of length Δx. The number of such segments $J = X/\Delta x$. A suitable time interval Δt is selected[1]. Define $s = \Delta t/\Delta x$. For a general function $f(x, t)$, let f_j^k denote the value of f at the point $(j\Delta x, k\Delta t)$ as shown in Figure 2.

Given $\{y_j^k, q_j^k\}_{j=0}^J$, we want to compute $\{y_j^{k+1}, q_j^{k+1}\}_{j=0}^J$. The update equations for $\{y_j^{k+1}, q_j^{k+1}\}_{j=1}^{J-1}$ are

$$y_j^{k+1} = a_{1j}y_{j-1}^k + b_{1j}y_{j-1}^k + c_{1j}y_j^k$$
$$+ d_{1j}q_j^k + e_{1j}y_{j+1}^k + f_{1j}q_{j+1}^k \tag{20}$$

$$q_j^{k+1} = a_{2j}y_{j-1}^k + b_{2j}y_{j-1}^k + c_{2j}y_j^k$$
$$+ d_{2j}q_j^k + e_{2j}y_{j+1}^k + f_{2j}q_{j+1}^k \tag{21}$$

and the update equations for y_0^{k+1} and y_J^{k+1} are

$$y_0^{k+1} = m_{10}y_0^k + m_{20}q_0^k + m_{30}y_1^k + m_{40}q_1^k + m_{50}u_0^k \tag{22}$$

$$y_J^{k+1} = m_{1J}y_{J-1}^k + m_{2J}q_{J-1}^k + m_{3J}y_J^k + m_{4J}q_J^k + m_{5J}p_J^k \tag{23}$$

A linear interpolation based procedure based on [13] is used for computing the coefficients a_{1j} through f_{1j}, a_{2j} through f_{2j}, m_{10} through m_{50} and m_{1J} through m_{5j}. The procedure is omitted here due to space limitations. It should be noted that the linear interpolation used in computing the coefficients introduces a dispersive character to the numerical

---

[1]For the numerical scheme to be convergent, the time step Δt should be selected such that the *Courant-Friedrichs-Lewy* (CFL) condition is satisfied: $\frac{\Delta t(|V_0|+C_0)}{\Delta x} < c$, with c, a constant, usually chosen to be 0.9. For explicit schemes, the CFL condition is also within a small factor of the stability condition.

1573

scheme [13]. However, the dispersion can be minimized by using sufficiently small time and space discretization steps. In the limit, the numerical solution will converge to the solution of the ODE system obtained with MOC (18,19) which is the exact solution of the linearized Saint-Venant PDE (8,9).

IV. ROBUST FEASIBILITY PROBLEM

A. Linear state-space model

From the MOC update equations (20,21,22,23), we obtain a state-space representation with state vector at time k defined by $\mathbf{x}(k) = (y_0^k, q_0^k, \ldots, y_J^k, q_J^k)^T$. The state evolution equation is

$$\mathbf{x}(k + 1) = A\mathbf{x}(k) + Bu(k) + Gp(k) \qquad (24)$$

with the applied control $u(k)$ in the form of discharge perturbation at the upstream end q_0^k and the discharge perturbation $p(k)$ at the downstream end q_J^k. The observation equation is

$$z(k) = C\mathbf{x}(k) \qquad (25)$$

with the stage perturbation $z(k) = y_J^k$ at the downstream end. Due to initial conditions given by equation (16), the initial state vector satisfies $\mathbf{x}(0) = 0$ and hence, $z(0) = 0$. We define the control and disturbance vectors up to (and excluding) time k by $\mathbf{u} = (u(0), \ldots, u(k - 1))^T$ and $\mathbf{p} = (p(0), \ldots, p(k - 1))^T$. Using equations (24,25), the output vector $\mathbf{z} = (z(1), \ldots, z(k))^T$ up to time k can be expressed as[2]

$$\mathbf{z} = \mathbf{A}\mathbf{p} + \mathbf{B}\mathbf{u} \qquad (26)$$

with $\mathbf{A}$ and $\mathbf{B}$ being lower-triangular, Toeplitz matrices with k-th row given by $(CA^{k-1}B, \ldots, CB, 0, \ldots, 0)$ and $(CA^{k-1}G, \ldots, CG, 0, \ldots, 0)$ respectively.

B. Admissible sets and problem statement

We consider the situation in which the control vector $\mathbf{u}$ and the disturbance vector $\mathbf{p}$ in equation (26) are unknown but bounded. That is, we require $\mathbf{u} \in \mathcal{U}$ and $\mathbf{p} \in \mathcal{P}$ where $\mathcal{U}$ and $\mathcal{P}$ are known, bounded sets that define the set of admissible control and disturbance trajectories up to (and excluding) time k. The requirement $\mathbf{p} \in \mathcal{P}$ is motivated by unknown demands at the downstream end. The requirement $\mathbf{u} \in \mathcal{U}$ is motivated by admissible discharge releases at the upstream end. We describe the set of admissible control trajectories by a polytopic model:

$$\mathcal{U} = \{\mathbf{u} : \|\mathbf{u}\|_\infty \leq \sigma_0\} = \{\mathbf{u} : \mathbf{U}\mathbf{u} \preceq \sigma\} \qquad (27)$$

with $\sigma \in \mathbb{R}_+^{2k}$ is a vector of σ_0's and $\mathbf{U} = (\mathbf{I}, -\mathbf{I})^T$, $\mathbf{I}$ the $k \times k$ identity matrix. Similarly, the set of admissible disturbance trajectories is modeled by

$$\mathcal{P} = \{\mathbf{p} : \|\mathbf{p}\|_\infty \leq \rho_0\} = \{\mathbf{p} : \mathbf{P}\mathbf{p} \preceq \rho\} \qquad (28)$$

with $\rho \in \mathbb{R}^{2k}$ and $\mathbf{P} = (\mathbf{I}, -\mathbf{I})^T$. We define the output feasible set $\mathcal{Z}$ as the set of all admissible output trajectories[3] up to time k:

$$\mathcal{Z} = \{\mathbf{z} : \|\mathbf{z}\|_\infty \leq \tau_0\} = \{\mathbf{z} : \mathbf{Z}\mathbf{z} \preceq \tau\} \qquad (29)$$

with $\tau \in \mathbb{R}_+^{2k}$ and $\mathbf{Z} = (\mathbf{I}, -\mathbf{I})^T$.

Definition 1: (Robustly feasible control). An admissible control trajectory $\mathbf{u} \in \mathcal{U}$ is robustly feasible if and only if for every admissible disturbance trajectory $\mathbf{p} \in \mathcal{P}$, the output trajectory of system (26) remains admissible, that is, $\mathbf{z} \in \mathcal{Z}$. We now give the problem statement.

Problem 1: (Robust feasibility problem). Find necessary and sufficient conditions for existence of a robustly feasible control trajectory for system (26) with sets of admissible control, disturbance and output trajectories defined by (29),(28),(29) respectively. That is, the problem is to find if there exists $\mathbf{u} \in \mathcal{U}$ such that for all $\mathbf{p} \in \mathcal{P}$, $\mathbf{z} = \mathbf{A}\mathbf{p} + \mathbf{B}\mathbf{u} \in \mathcal{Z}$.

C. Solution of robust feasibility problem using LP duality

We first state a lemma which follows from LP duality.

Lemma 1: Given a vector $\mathbf{v}$, and a scalar δ, the condition $\mathbf{v}^T\mathbf{p} \leq \delta$ for every $\mathbf{p} \in \mathcal{P}$ is satisfied if and only if there exists λ such that

$$\lambda \succeq 0, \mathbf{P}^T\lambda = \mathbf{v}, \lambda^T\rho \leq \delta.$$

Proof: $\mathbf{v}^T\mathbf{p} \leq \delta \, \forall \mathbf{p} \in \mathcal{P} \Leftrightarrow \delta \geq \max_{\mathbf{p}}\{\mathbf{v}^T\mathbf{p} : \mathbf{P}\mathbf{p} \leq \rho\} = \min_{\lambda \succeq 0}\{\lambda^T\rho : \mathbf{P}^T\lambda = \mathbf{v}\} \Leftrightarrow \exists \lambda \succeq 0, \mathbf{P}^T\lambda = \mathbf{v}, \lambda^T\rho \leq \delta.\square$

Consider the case when the control $\mathbf{u}$ in system (26) is fixed. Without loss of generality, we can set $\mathbf{u} = 0$. Problem 1 reduces to checking whether

$$\forall \mathbf{p} \in \mathcal{P}, \quad \mathbf{z} = \mathbf{A}\mathbf{p} \in \mathcal{Z} \qquad (30)$$

The following corollary follows directly by applying Lemma 1 row-wise to condition $\mathbf{Z}\mathbf{z} = \mathbf{Z}\mathbf{A}\mathbf{p} \preceq \tau$.

Corollary 1: Condition (30) holds if and only if

$$\exists \mathbf{M} = (m_{ij}) : m_{ij} \geq 0 \; \mathbf{P}^T\mathbf{M} = \mathbf{A}^T\mathbf{Z}^T, \mathbf{M}^T\rho \preceq \tau \quad (31)$$

The above corollary can be generalized to the case of feedforward control. Here, we let $\mathbf{u}$ to be a variable and the robust feasibility problem is:

$$\text{Find } \mathbf{u} : \mathbf{u} \in \mathcal{U}, \forall \mathbf{p} \in \mathcal{P}, \mathbf{A}\mathbf{p} + \mathbf{B}\mathbf{u} \in \mathcal{Z} \qquad (32)$$

Again, applying Lemma 1 row-wise to condition $\mathbf{Z}(\mathbf{A}\mathbf{p} + \mathbf{B}\mathbf{u}) \preceq \tau$ we obtain the following necessary and sufficient conditions for condition (32) to hold:

$$\exists \mathbf{M} = (m_{ij}), \exists \mathbf{u} \; : \; m_{ij} \geq 0, \mathbf{U}\mathbf{u} \preceq \sigma,$$
$$\mathbf{P}^T\mathbf{M} = \mathbf{A}^T\mathbf{Z}^T, \mathbf{Z}\mathbf{B}\mathbf{u} + \mathbf{M}^T\rho \preceq \tau \quad (33)$$

Conditions (31) and (33) can be checked using linear programming. Note that condition (33) reduces to (31) when we impose $\mathbf{u} = 0$.

We now consider the case of affine disturbance feedback control. That is, we assume that the disturbance trajectory $\mathbf{p}$

---

[2]Note that the sizes of $\mathbf{A}, \mathbf{B}, \mathbf{z}, \mathbf{p}, \mathbf{u}$ depend on k. This dependence is omitted for notational convenience.

[3]Time varying admissible bounds can be incorporated by setting σ, ρ, τ as vectors of variable entries. For example, σ can be set as $(\sigma_1^+, \ldots, \sigma_k^+, \sigma_1^-, \ldots, \sigma_k^-,)^T$.
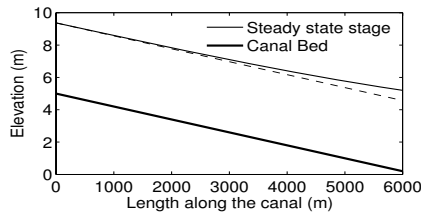
Fig. 3. Steady state stage profile.

Control Case	ρ_0	σ_0	τ_0
No control	0.0095	0.0	0.03
Feedforward	0.0095	0.0275	0.03
Feedback	0.02825	0.0275	0.03

TABLE I

Parameters describing admissible disturbance, control and stage trajectories.

is measured and the control trajectory **u** is an affine function of **p**. Specifically,

$$\mathbf{u(p)} = \mathbf{u} + \mathbf{Lp} \qquad (34)$$

In order to impose that control is affine function of *past* disturbances, we impose **L** to be lower triangular matrix.

Remark 2: This type of control parameterization has been used in robust model predictive problems [14]. In [14], the authors show that control parameterization (34) is equivalent to the one where the control is affine function of past states. The advantage of using (34) is that the robust feasibility problem can be solved using a tractable and convex problem. The robust feasibility problem in this case is:

Find **u** and **L** lower-triangular :

$$\forall \mathbf{p} \in \mathcal{P}, \mathbf{u} + \mathbf{Lp} \in \mathcal{U}, \mathbf{Ap} + \mathbf{B(u + Lp)} \in \mathcal{Z} \qquad (35)$$

This problem can be solved in two steps. First, the admissibility of function **u(p)** is considered in the sense that $\mathbf{u(p)} = \mathbf{u} + \mathbf{Lp} \in \mathcal{U}$ for every $\mathbf{p} \in \mathcal{P}$. According to our previous development, this is guaranteed by the following necessary and sufficient condition.

$$\exists \mathbf{N} = (n_{ij}), \exists \mathbf{u}, \exists \mathbf{L} \text{ lower-triangular} :$$
$$n_{ij} \geq 0, \mathbf{P}^T \mathbf{N} = \mathbf{L}^T \mathbf{U}^T, \mathbf{Uu} + \mathbf{N}^T \rho \preceq \sigma \qquad (36)$$

In the second step, for a fixed **u** and **L**, the admissibility of output **z** is considered in the sense that $\mathbf{Ap} + \mathbf{B(u + Lp)} \in \mathcal{Z}$ for every $\mathbf{p} \in \mathcal{P}$. This is guaranteed by the following necessary and sufficient condition

$$\exists \mathbf{M} = (m_{ij}) :$$
$$m_{ij} \geq 0, \mathbf{P}^T \mathbf{M} = (\mathbf{A} + \mathbf{BL})^T \mathbf{Z}^T, \mathbf{ZBu} + \mathbf{M}^T \rho \preceq \tau \qquad (37)$$

Again, the conditions (36,37) are affine inequalities in decision variables **M, N, L, u** and can be checked using linear programming. These conditions reduce to (33) when we impose **L** = 0.

V. CASE STUDY

This section deals with solving the robust feasibility problem for the case of a representative dam-reservoir system. The parameters of equations (1,2,3) are summarized as follows: $T = 8\ m$, $S_b = 0.0008\ m/m$, $n = 0.02\ m^{-1/3}s$, $w = 0\ m^2/s$. Equations (4,5) are solved for $Q_0 = 80\ m^3/s$ and $Y_0(X) = 5\ m$. The steady state discharge profile is constant and the steady state stage profile is plotted in Figure 3. It can be checked that the flow is sub-critical.

Let us recall that the original control problem: For system (1,2), regulate the upstream discharge $Q(0,t)$ such that under the effect of downstream perturbation $Q(X,t)$, the downstream stage $Y(X,t)$ stays within a desired range. Under the assumption of small deviations around the steady state, the solution of the original nonlinear system can be approximated by the solution of the linear system (8,9,15,16) plus the steady state solution. The control problem now becomes that of controlling the upstream discharge deviation $q(0,t)$ such that under small perturbations in downstream boundary condition $q(X,t)$, the downstream stage deviation $y(X,t)$ remains sufficiently close to 0. We implement the MOC based numerical scheme of Section III in MATLAB for the space step $\Delta x = 300\ m$. Using the CFL condition, the time step of $\Delta t = 30\ s$ is chosen. The total time horizon of $3600\ s$ is chosen and thus, number of time intervals is $K = 120$. Using procedure outlined in Section IV-A, matrices **A** and **B** of equation (26) are constructed.

The polytope $\mathcal{Z}$ that models the admissible set of output trajectories is defined by setting the vector τ as the constant vector with entries $\tau_0 = 0.03$ (see equation (29)). This requirement imposes the constraint that the downstream stage deviation $y(X, k\Delta t)$ must remain within $\pm 0.15\ m$ ($\pm 3\%$ of $Y_0(X)$) throughtout the time horizon. We solve the robust feasibility problem (see Section IV) for the case without control, and for the cases of feedforward and disturbance feedback controls. The conditions for existence of a robustly feasible solution for each of the three cases are respectively given by equations (31), (33) and (36,37). These conditions can be checked using standard LP solvers. In this study the MINOS solver is used.

For the case of feedforward and of disturbance feedback control, the polytope $\mathcal{U}$ that models the admissible set of control trajectories is defined by setting the vector σ as the constant vector with entries $\sigma_0 = 0.0275$ (see equation (27)). This requirement imposes the constraint that the upstream hydraulic structure can be regulated around the steady state operating point to release $\pm 2.2\ m^3/s$ ($\pm 2.75\%$ of Q_0) of water in the canal. The polytope $\mathcal{P}$ that models the set of admissible disturbance trajectories is also defined by setting the vector ρ as the constant vector with entries ρ_0. By increasing the value of ρ_0, the set of admissible disturbance trajectories becomes larger. Starting from small ρ_0, the set $\mathcal{P}$ is systematically increased until the conditions for existence of robustly feasible solution are no longer feasible. For each of the three cases, the maximum value of ρ_0 for which these conditions remain feasible are reported in Table I.

For the case of without control (see (31)) and of feedforward control (see (33)), increasing ρ_0 beyond 0.0095 made the feasible region of the LP problem unbounded. Thus, the
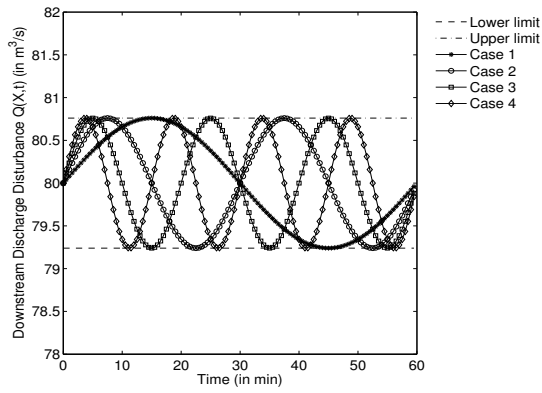
1575

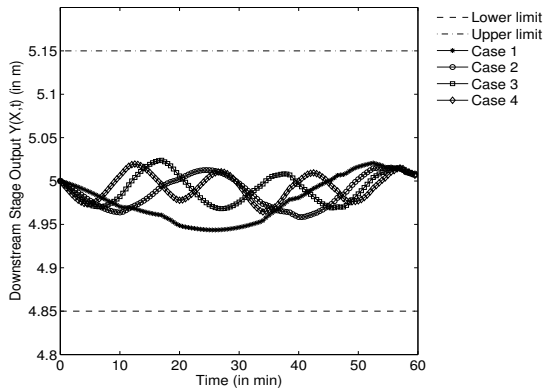Fig. 4.　Disturbance for feedforward case with and without constraint on **u**.

Fig. 5.　Output for feedforward case with and without constraint on **u**.

Fig. 6.　Control for feedforward case without constraint on **u**.

Fig. 7.　Disturbance for feedback case with and without constraint on **u**.

maximum admissible disturbance that can be imposed by the users at the downstream end of the canal without compromising on the robust feasibility is $\pm 0.76 \ m^3/s$ (0.95% of Q_0). In this particular study, the feedforward control did not increase the admissible set of disturbance trajectories. For the case of disturbance feedback, the corresponding maximum admissible disturbance is $\pm 2.26 \ m^3/s$ (2.825% of Q_0).

In order to test the performance of feedback control and feedforward control, four different trajectories of admissible disturbances are considered: $p_0(t) = Q_0 \sin\left(\frac{i\pi\rho}{K}t\right)$ with $i = 2, 4, 6$ and 8. For the case of feedforward control, each of the admissible disturbances are simulated (see Figure 4). The resulting output and input trajectories are shown in Figure 5 and Figure 6 respectively.

For the case of feedback control (see (36,37)), the disturbance, output and input trajectories are shown in Figure 7, Figure 8 and Figure 9 respectively. It can be observed from the figures that for each of the disturbance, the control and output trajectories remain admissible throughout the time horizon[4].

From Figure 6 and Figure 9, one can observe that the robustly feasible input trajectories seem to fluctuate more than that might be desirable from a point-of-view of upstream

gate operation. This issue can be addressed by imposing additional constraints while solving the problems (33) and (36,37). We impose the following constraint

$$|u(k+1) - u(k)| \leq \epsilon \qquad (i = 1, \ldots, K-1) \qquad (38)$$

where, ϵ is the maximum allowable discharge fluctuation between two consecutive time steps. We choose $\epsilon = 0.1 \ m^3/s$. Problems (33) and (36,37) are again solved with constraint (38) imposed. The robustly feasibly input trajectories for feedforward and feedback case are shown in Figure 10 and Figure 11 respectively. It is observed that the admissible

Fig. 8.　Output for feedback case with and without constraint on **u**.

---

[4]As observed in Figure 8, the output trajectory deviates slightly from the admissible bound for the case when $i = 2$. This can be attributed to numerical errors.
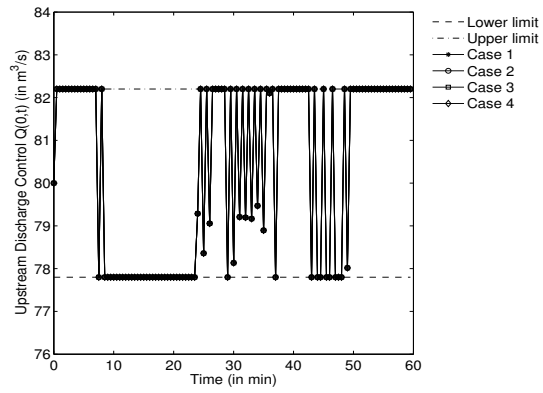
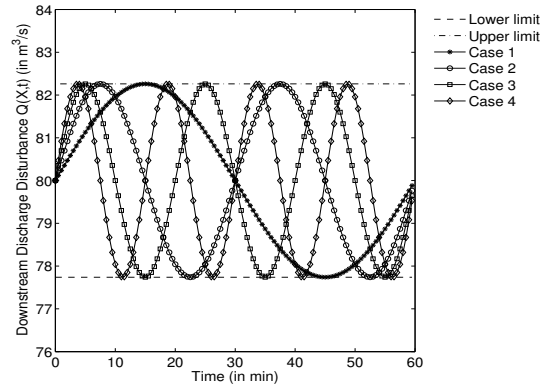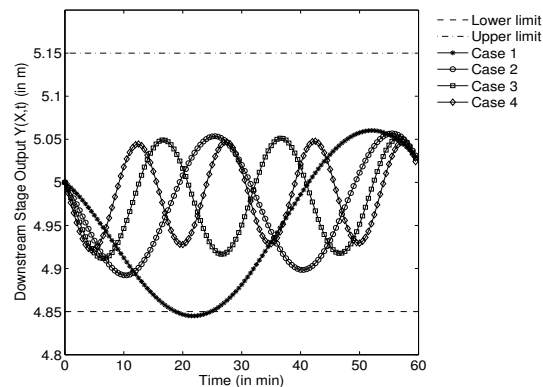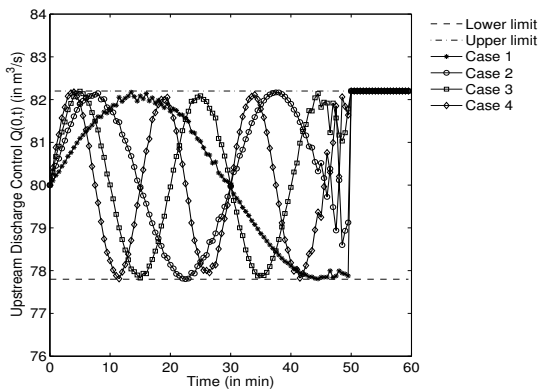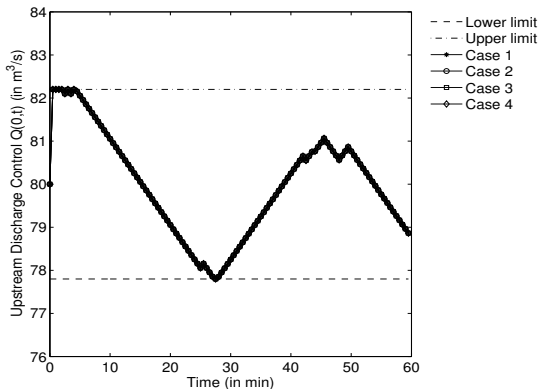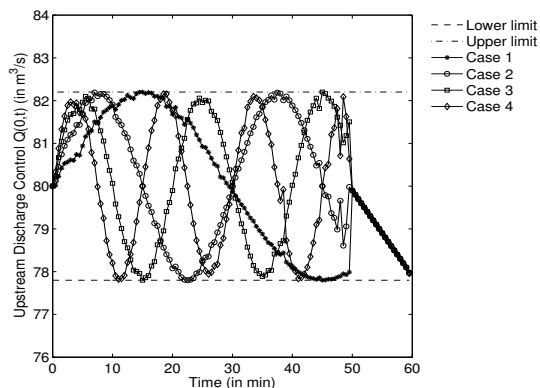Fig. 9. Control for feedback case without constraint on **u**.

Fig. 10. Control for feedforward case with constraint on **u**.

set of robustly feasible input trajectories does not reduce for the constrained problems. However, the input trajectories are more desirable from an operational viewpoint. It can be noticed from Figure 10 that feedforward control has a tendency to switch between one extreme to another. Lastly, toward the end of time horizon, the feedback control trajectories in Figure 11 show some abrupt variations before they start behaving like open loop trajectories. This may be partly attributed to finite-horizon problem structure of the problem.

Fig. 11. Control for feedback case with constraint on **u**.

VI. CONCLUSION AND FUTURE WORK

This article showed that the robust distant downstream control problem for a reservoir-canal system can be formulated as a robust feasibility problem in which the constraints on admissible set of disturbance, control and output trajectories can be easily incorporated. The resulting necessary and sufficient conditions are affine in the control variables and can be checked in a computationally efficient manner using standard LP solvers.

The discussion in the article is concentrated on upstream discharge as the control variable. For practical implementation, the upstream discharge needs to be translated to gate openings. This can be done by incorporating the stage-discharge rating curve of the upstream hydraulic structure in the problem formulation. When certain operational constraints are relaxed, introduction of soft constraints can lead to better solutions [9]. The admissible set of trajectories can be also be allowed to be time varying by appropriately modifying the polytopes. Lastly, longer time intervals can be taken into consideration. Practical considerations such as these will be addressed in future work. Future work will also focus on robust model predictive control [14], with application to canal control.

REFERENCES

[1] C. Burt and S. Styles, "Modern water control and management practices in irrigation," Tech. Rep., 1999, technical report, FAO, IPTRID, World Bank.
[2] P. Malaterre, D. Rogers, and J. Schuurmans, "Classification of canal control algorithms," *ASCE Journal of Irrigation and Drainage Engineering*, vol. 124, no. 1, pp. 3–10, 1998.
[3] J. Cunge, F. Holly, and A. Verwey, *Practical aspects of computational river hydraulics*. Pitman, 1980.
[4] X. Litrico and V. Fromion, "Tuning of robust distant downstream PI controllers for irrigation canal pool: (i) theory," *ASCE Journal of Irrigation and Drainage Engineering*, vol. 132, no. 4, pp. 359–368, 2006.
[5] P. Malaterre and M. Khammash, "ℓ_1 controller design for a high-order 5-pool irrigation canal system," *Journal of Dynamic Systems Measurement and Control*, vol. 125, no. 4, pp. 639–645, 2003.
[6] X. Litrico and V. Fromion, "$\mathcal{H}_\infty$ control of an irrigation canal pool with a mixed control politics," *IEEE Transactions on Control Systems Technology*, vol. 14, no. 1, pp. 999–111, 2006.
[7] P. Malaterre, "Pilote: Linear quadratic optimal controller for irrigation canals," *ASCE Journal of Irrigation and Drainage Engineering*, vol. 124, no. 4, pp. 187–194, 1998.
[8] A. Garcia, M. Hubbard, and J. de Vries, "Open channel transient flow control by discrete time LQR methods," *Automatica*, vol. 28, no. 2, pp. 255–264, 1992.
[9] G. Hug-Glanzmann, M. von Siebenthal, T. Geyer, G. Papafotiou, and M. Morari, "Supervisory water level control for cascaded river power plants," in *Hydropower Conference 05*, Stavanger, Norway, 2005.
[10] J. de Halleux, C. Prieur, B. Andrea-Novel, and G. Bastin, "Boundary feedback control in networks of open channels," *Automatica*, vol. 39, no. 8, pp. 1365–1376, 2003.
[11] M.-L. Chen and D. Georges, "Nonlinear optimal control of an open-channel hydraulic system basedon an infinite-dimensional model," in *Proceedings of the 39th Conference of Decision and Control*, Phoenix, USA, 1999, pp. 4313–4318.
[12] X. Litrico and V. Fromion, "Frequency modeling of open channel flow," *ASCE Journal of Journal of Hydraulic Engineering*, vol. 130, no. 8, pp. 806–815, 2004.
[13] E. Wylie and V. Streeter, *Fluid Transients*. McGraw Hill Book Company, 1978.
[14] P. Goulart, E. Kerrigan, and J. Maciejowski, "Optimization over state feedback policies for robust control with constraints," *Automatica*, vol. 42, no. 4, pp. 523–533, 2006.